The Florida Current at Key West: Summer 1972

by Irving H. Brooks[1] and Pearn P. Niiler[2]

ABSTRACT

Sixteen dropsonde cross-sections of the Florida Straits at the Key West, Florida, longitude are used to examine the persistent features and large-scale variations of the temperature, salinity, and horizontal velocity structures of the Florida Current. A persistent counterflow was found along the northern shore of the Current, which can be interpreted from the salinity distribution as cyclonic recirculation of the Florida Current water. Analysis of the temporal variations indicate that a downstream acceleration of the Current is accompanied by a warming trend.

1. Introduction

During the spring and summer of 1972, a concerted observational program was conducted on the influx and efflux of the Loop Current in the Gulf of Mexico. Nova University monitored the transport across sections at Yucatan and Key West by air dropsondes. The section south of Key West was also monitored by the R/V Gulf Stream, which deployed a freely dropped STD as well as boat dropsondes. In addition, NOAA's R/V Virginia Key carried out a hydrographic survey at Yucatan, and the University of Miami occupied two profiling current meter stations south of Key West for 13 days. During the intensive survey at the exit and entrance of the Gulf of Mexico, Texas A & M University's R/V Alaminos engaged in mapping the Loop Current. The total observational program was geared toward monitoring the variables which are useful as input to a seasonally persistent numerical model of the Loop Current.

This paper is a description and analysis of the shipboard measurements from the Key West location and represents the first report on direct simultaneous measurements of the current and density fields of the Florida Current at this location. Herein we present the ensemble average profiles of the directly measured horizontal velocity, temperature, and salinity, and discuss the structure of the variations of the Current during this early summer period.

2. Scope of the experiment

Between May 3 and June 8, 1972, 16 cruises were made across the Florida Current, along the 81°44′4″W meridian between Key West, Florida, and Matanzas, Cuba

1. Nova University, Fort Lauderdale, Florida, 33004, U.S.A.
2. Department of Oceanography, Oregon State University, Corvallis, Oregon, 97331, U.S.A.

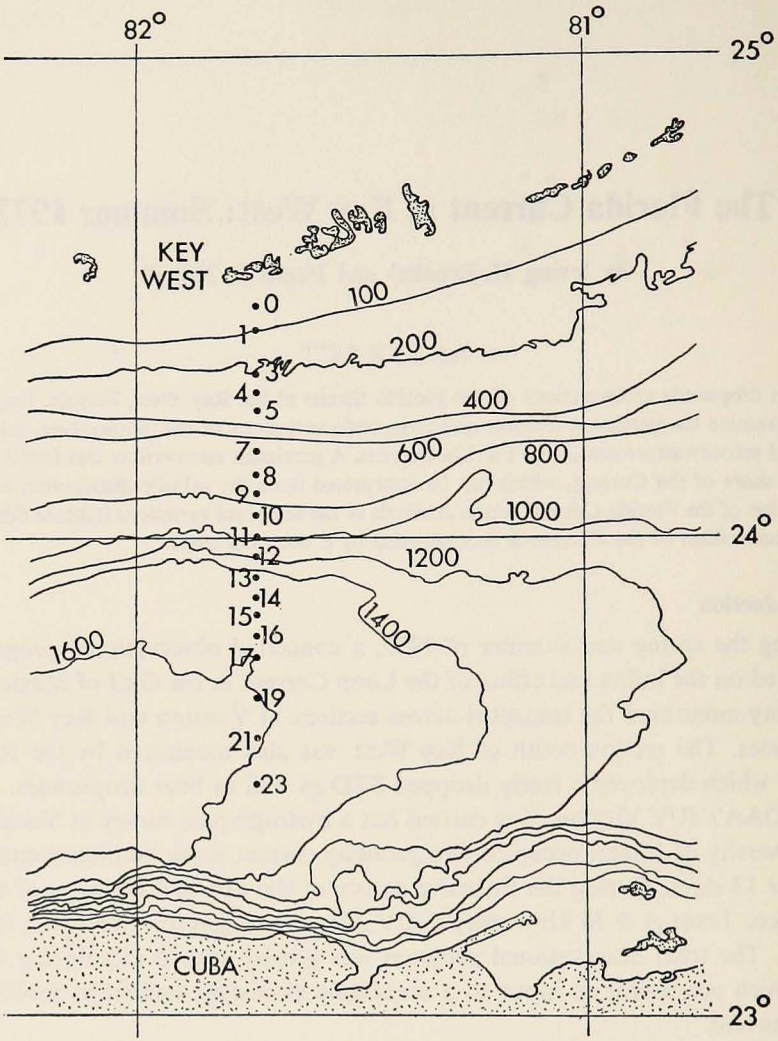

Figure 1. The experimental section.

(see Figure 1 and Table I). All transport measurements were made with freely falling dropsondes, as described by Richardson and Schmitz (1965), and containing modifications discussed by Richardson, Carr, and White (1969). Upon reaching a station, dropsondes were sent to pre-selected depths, usually at intervals of 100 to 200 meters. The number of instruments used at a particular station was determined by the depth of the station. Temperature and salinity measurements were made with a Bissett-Berman Model 9060 STD, which was incorporated into the deepest-running dropsonde. This self-contained STD renders a continuous record of temperature and salinity vs. depth throughout its travel. Although the depth of the ocean floor was

Table I. Scope of the Experiment.

STATION NO.	0	1	3	4	5	7	8	9	10	11	12	13	14	15	16	17	19	21	23	Transport†
DATE																				
May 3.....	S	T	*	*	*	*	*	*		*	*	*		T	*	*	*	*	*	20.3
May 5.....			*		*	*	*													
May 9.....			*		*	*	*	*	*	*	*	*	*	*		*	*	*	T	20.4
May 11.....			*		T	T	*	*	*	*	*	*	*	*		*	*	*	*	22.5
May 13.....			*		*	*	*	*	*	*	T		T							
May 17.....					T	*	*		*		*	*	*	*		*	*	*	*	16.9
May 19.....													T	T		T	*	*	*	
May 21.....	S		T		T	T	T	T	T	T		T		T		T	T	T	T	21.3
May 24.....	S		*		*	*	*	T	*	*		*		*		*	*	T	*	20.9
May 27.....	S		T		T	T	*	*	T	*		*		*		*	*	*	*	19.2
May 29.....			*		*	*	T	*	T	T		*		T		T	T	T	T	19.1
May 31.....	S		T		T	T	T	T	T	T		T		*		*	*	*	*	21.2
June 2.....	S		*		*	T	*	*	*					*		*	*	*	*	23.2
June 4.....	S		*		*	*	T	*	*	T		*		*		*	*	*	*	23.7
June 6.....	S		T		T	T	T	T	T	T		T		T		T	T	T	T	24.8
June 8.....	S		*		*	*	*	*	*	*		*		*		*	*	*	*	24.6

† $10^6 m^3$/sec (from surface to $\bar{\sigma}_t = 27.0$ and not including water within 35 kilometers of Cuba).
* Surface current, transport, and STD measurements.
T Surface current and transport measurements only.
S Surface current measurement only.
Total number of surface current measurements = 201
Total number of transport measurements = 192
Total number of STD measurements = 130.

as great as 1600 meters at some locations in the section, measurements were made only to depths of 1000 meters due to STD depth limitations.

Past performances of this STD have shown the temperature sensor to be quite reliable ($\pm .05°C$), but, in deep water, salinity values have been recorded which are as much as $0.6‰$ lower than historical salinity data in this region. During these observations, deep-water salinity values were frequently recorded which were lower than the historical data by $0.15‰$. On these occasions, the entire salinity profile was adjusted so that the deep-water value was $34.75‰$. This is the minimum historical value for the South Atlantic water below 500 m.

At every 25 meters of depth, σ_t was calculated from the temperature and salinity data. Over the range of temperatures and salinities encountered, σ_t was a much stronger function of temperature than of salinity. The salinity recalibration described above had a minimal effect on the calculated σ_t values.

The transport data requires somewhat more manipulation than the STD data. The measured quantity is transport, or average velocity (transport/depth), from which it is desired to find the actual velocity profile. First the vector measurement was decomposed into downstream (west-to-east) and cross-stream (south-to-north) components. For each component, $u(z) = \dfrac{d}{dz}(zU(z))$, where $u(z)$ is velocity at depth z

and $U(z)$ is average velocity (the measured quantity) to depth z. It is beneficial to have an analytic expression for $U(z)$ so that $u(z)$ can be computed for any z. This is obtained by fitting a curve through the measured points. At most, we had five measurements of $U(z)$ for a single occupation of a station, as opposed to a minimum of three measurements which occurred only at the shallow-water stations (less than 250 m. depth). After evaluating several curve-fitting techniques, it was decided that smoothing spline functions, as described by Reinsch (1967) gave the most realistic results. The main advantage of this method was that the curvature was minimized and a different third degree polynomial represented the curve between consecutive data points. When a single function was used to fit the data over the entire depth interval, unrealistic values of the velocity were obtained in the deep water. It is interesting to note that no such distinction is evident if only ensemble-averaged velocity values are desired. For this situation, there is virtually no difference between results derived from spline fits and those from least-squares polynomial fits. This suggests that some vertical scales of the "instantaneous" velocity structure are lost in the averaging process. One such feature is a subsurface downstream velocity maximum, which is apparent in the daily contour plots but is not present in the average field.

After velocity components and σ_t values were calculated, ensemble-averaged profiles of temperature, salinity, σ_t, and velocity were calculated for the 13 stations that were repeatedly occupied. Deviations from these means were then derived for each occupation of each station.

3. Average properties

Figure 2 shows the ensemble-averaged profiles of $U(z)$, $V(z)$ (average velocity to depth z of downstream and cross-stream components, respectively), T temperature), and S (salinity) for Station 9. All the data points, from which the ensemble averages were determined, are included in the figure. This data, which is typical of that of any of the stations, shows the wide range of scatter in the transport measurements as compared to the STD measurements. The ensemble average curves are drawn only to the depths to which all profiles contribute to the average. This is the minimum value to which the deepest instrument traveled at this station during the entire experiment. Due to occasional STD malfunctions, there are more transport profiles than temperature and salinity profiles.

Figure 3 shows the cross-sectional contours of average downstream velocity. Note the region of counterflow in the northern part of the section. This is the first time that a persistent sizable counterflow was observed in the Straits of Florida using free-fall instruments (vide Richardson, Schmitz, and Niiler (1969)), although Düing and Johnson (1971, 1972) describe the occasional occurrence of similar features under the western edge of the Florida Current at a section between Miami and Bimini. The counterflow was discerned in this region for all but three of the cruises.

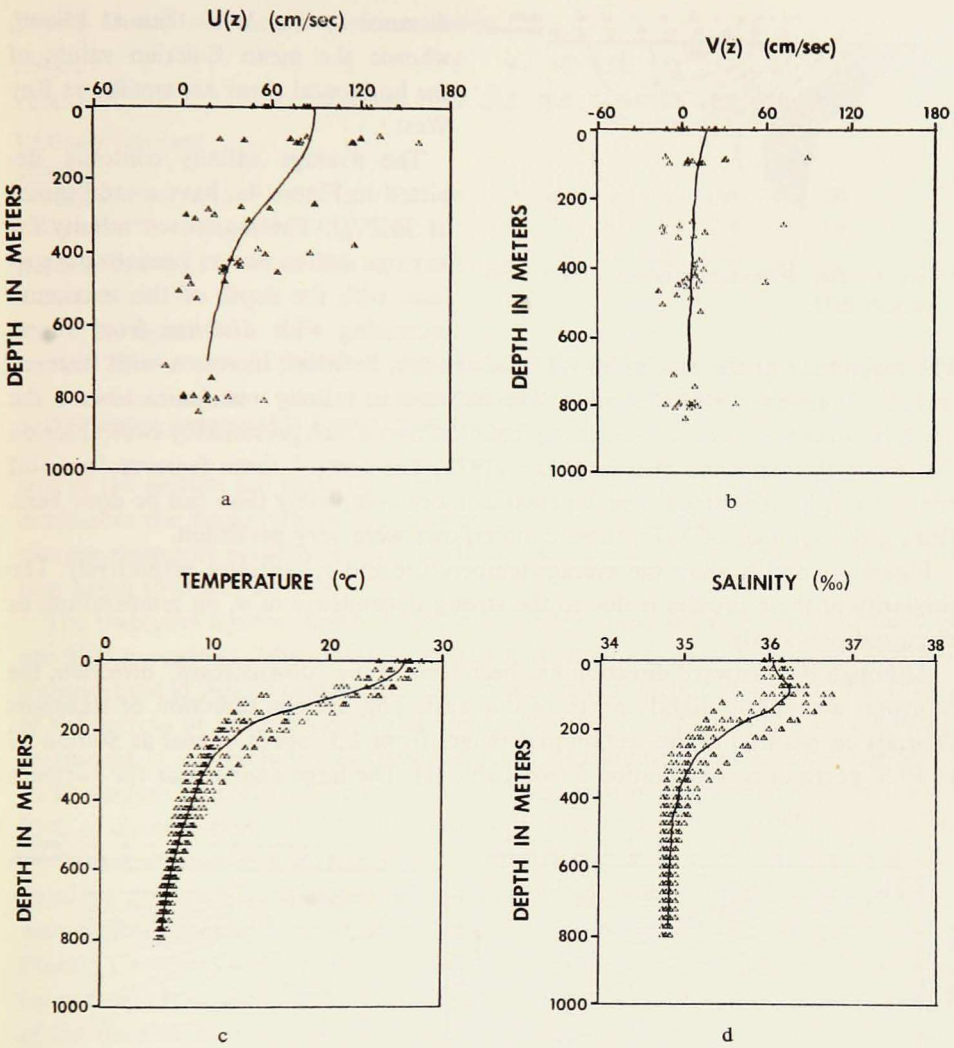

Figure 2. The data ensemble for Station 9: (a) downstream average velocity, $U(z)$; (b) cross-stream average velocity, $V(z)$; (c) temperature; (d) salinity.

For the ensemble-averaged fields, the velocity in the counterflow reached as high as 25 cm/sec. The maximum velocity in the downstream-flowing portion of the section was 145 cm/sec. Note also the relatively weak horizontal cyclonic shear of this section as compared to other sections across the Florida Current (Richardson, Schmitz, and Niiler (1969)). The surface value is roughly $.26+10^{-4}$ sec^{-1} at this section, as compared with the Miami Section of $.57+10^{-4}$ sec^{-1}. Daily plots (Fig. 6a, 6b) showed that instantaneous values of the cyclonic shear at the Key West section were as large as the instantaneous values at Miami. The Florida Current meanders over a larger

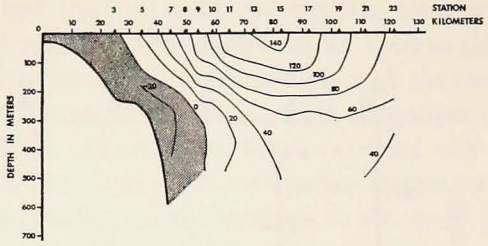

Figure 3. The ensemble-averaged downstream velocity field.

distance at Key West than at Miami, whence the mean Eulerian values of the horizontal shear are smaller at Key West.

The average salinity contours, depicted in Figure 4a, have a saddlepoint at $36.2^{0}/_{00}$. The maximum salinity for any one station occurs beneath the surface, with the depth of this maximum increasing with distance from shore. The magnitude of the maximum value of salinity, however, increases with distance in both directions from Station 7. The increase in salinity maximum toward the north is directly associated with strong counterflows which presumably sweep Florida Current water into the shallows. Lee (1972) has termed these features "spin-off eddies" and has described their kinematics more completely than can be done here. During the summer of 1972, these counterflows were very persistent.

Figures 4b and 4c show the average temperature and σ_t contours, respectively. The similarity of these profiles is due to the strong dependence of σ_t on temperature, as discussed previously.

Although the eastward direction has been termed the "downstream" direction, the transport actually is slightly north of due east. The average direction of transport depends on position in the section and ranges from 2.3° north of east at Station 15 to 19.5° north of east at Station 5 (see Table II). The large angles near the northern

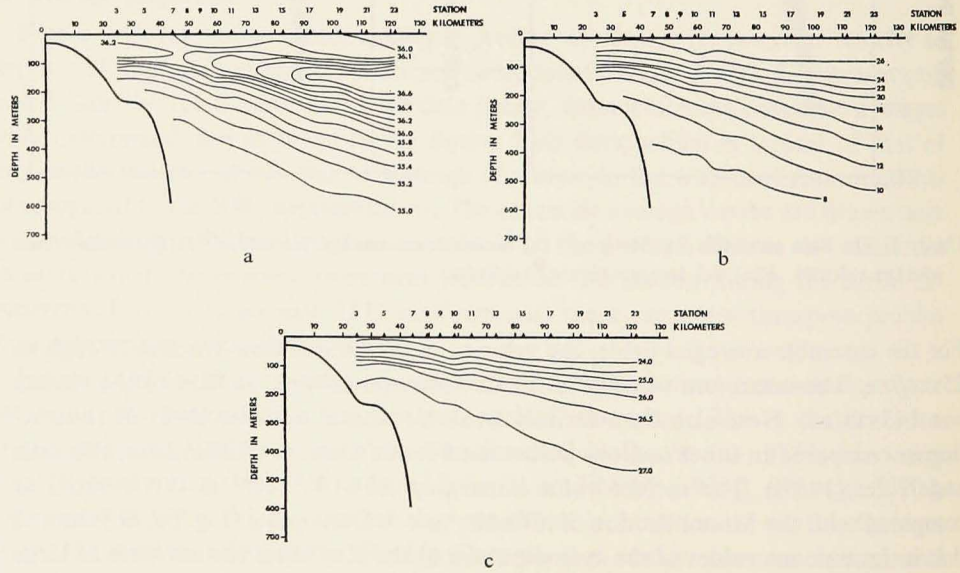

Figure 4. The ensemble-averaged hydrographic fields: (a) salinity, (b) temperature, (c) σ_t.

Table 2. Ensemble-averaged properties vs. station.

Station	3	5	7	8	9	10	11	13	15	17	19	21	23
Position*.....	25.1	34.6	44.4	49.3	54.2	59.0	64.0	73.4	83.2	92.8	102.8	112.3	122.1
Vertically Averaged Velocity													
Mag. (cm/sec)....	8	9	31	44	62	71	91	99	100	91	80	69	57
Direction**.....	165.5	19.5	13.5	13.5	6.5	7.4	5.1	3.5	2.3	3.2	2.9	3.3	3.0
Depth of 27.0 $\bar{\sigma}_t$.... (meters)	160	140	175	205	230	235	270	280	335	370	420	450	460
Avg. $\bar{\sigma}_t$ for water above 27.0 $\bar{\sigma}_t$.....	25.69	25.51	25.58	25.58	25.58	25.42	25.65	25.53	25.60	25.61	25.67	25.66	25.64

* Distance (kilometers) south of 24°33′56.0″N latitude along 81°44′4.0″W meridian.
** Direction is measured in degrees counterclockwise from due east.

end of the section are partially due to the counterflow, previously discussed, which diminishes the magnitude of the eastward transport. For Station 3, the direction of average transport actually is 14.5° north of west, the east-west transport at this station being towards the west.

The transport figures shown in Table I give the transport only down to the average 27.0 σ_t contour, which was arbitrarily chosen as a bottom boundary. The total transport could not be calculated, since measurements were not made to the bottom of the section at all stations. Water transported below this level or to the south of Station 23 is not included in these figures. (Measurements were not made within 35 kilometers of Cuba.) The ensemble average transport reported here is roughly 75% of the transport noted by Richardson, Schmitz, and Niiler (1969), across a sectio between Marathon and Cay Sal Bank during the same months in 1966. The standard deviation for transport calculations was $2.3+10^6$ m^3 sec^{-1}, which compares with figures reported by Niiler and Richardson (1973) for other sections across the Florida Current. On Table II, we present the ensemble average data in a "two-layer" format, which would be most useful in numerical modeling studies of the circulation of the Gulf of Mexico.

4. Fluctuations

The deviations from the respective mean values of downstream velocity, cross-stream velocity, and σ_t were plotted for each occupation of each station. The series of graphs displayed in Figure 5 is for Station 9, which again was chosen for display purposes. Only those cruises from which STD data was obtained are included here. The mean velocity profiles have been recalculated on this basis.

Density fluctuations were noted primarily in the upper 300 meters of the cross-section. This was particularly true in the cyclonic shear region (north of Station 13, according to ensemble-averaged figures), where the density fluctuations were largest in magnitude. A strong coherence existed here between fluctuations of density and

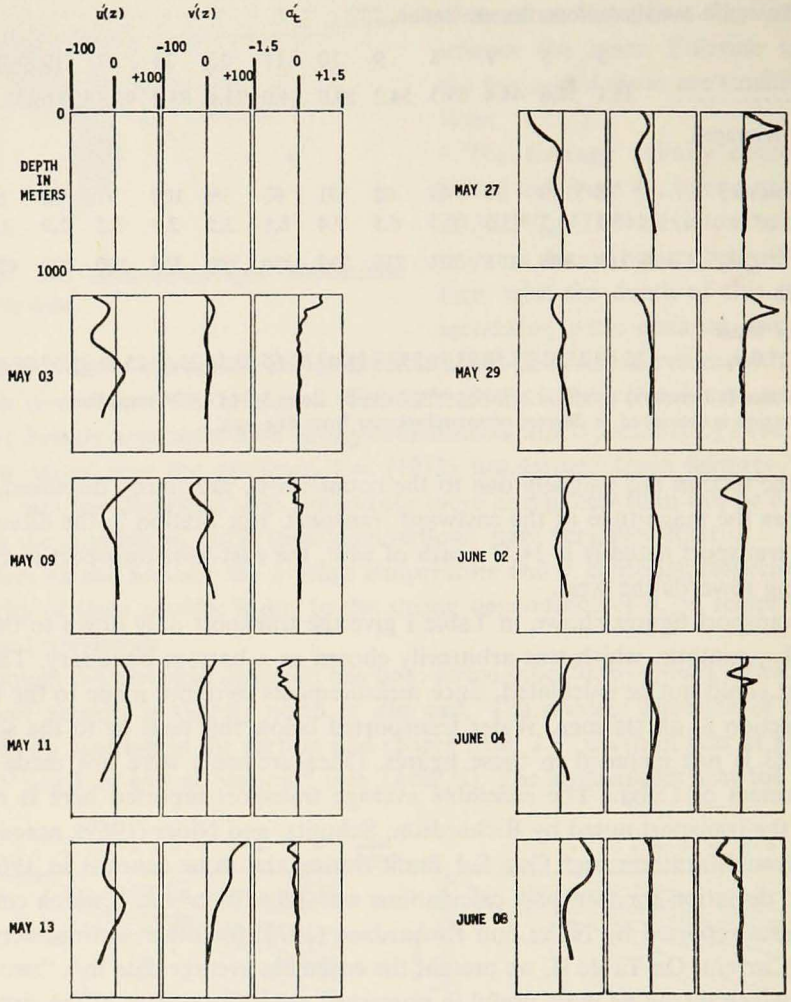

Figure 5. Fluctuations of velocity components and σ_t at Station 9.

downstream velocity. With primed quantities representing the deviations from the ensemble average of a quantity, and considering only the top 300 meters for Stations 3–13, the product $u'\sigma_t'$ was negative in 69% of the cases and positive in 16% of the cases, while for the remaining 15% of the cases, $u'\sigma_t' \approx 0$. Furthermore, for each of the individual stations $u'\sigma_t'$ was negative at least three times as often as it was positive. Thus, in the upper layer of the cyclonic shear region, an increase (decrease) in density is accompanied by a downstream deceleration (acceleration).

With reference to the fluctuation energy equation:

$$\frac{D}{Dt}\left[\frac{\overline{(u')^2}}{2}+\frac{\overline{(v')^2}}{2}+\frac{g}{\varrho_0}\frac{1}{|\partial\bar{\sigma}_t/\partial z|}\frac{\overline{(\sigma_t')^2}}{2}\right]=-\overline{u'v'}\frac{\partial\bar{u}}{\partial y}-\overline{v'\sigma_t'}\frac{g}{\varrho_0}\frac{\partial\bar{\sigma}_t/\partial y}{|\partial\bar{\sigma}_t/\partial z|}$$

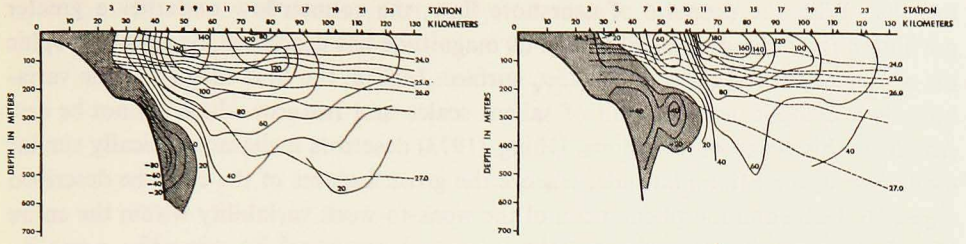

Figure 6. Two phases of the cyclonic region oscillations for which $u'\sigma_t' < 0$. Solid lines are isotachs and dotted lines are isopycbals. (a) a day when $u' > 0$ and $\sigma_t' < 0$ predominates; (b) a day when $u' < 0$ and $\sigma_t' > 0$ predominates.

$$-\overline{u'u'}\frac{\partial \bar{u}}{\partial x} - \overline{u'\sigma_t'}\frac{g}{\varrho_0}\frac{\partial \bar{\sigma}_t/\partial x}{|\partial \bar{\sigma}_t/\partial z|} - \overline{u'w'}\frac{\partial \bar{u}}{\partial z}$$

$$-\frac{1}{\varrho_0}\left[\overline{(u'p')_x} + \overline{(v'p')_y} + \overline{(w'p')_z}\right].$$

( ) represents an ensemble average, w is vertical velocity, x and y are the downstream and cross-stream directions, and $\dfrac{D}{Dt}$ is the derivative following the mean motion $\vec{\bar{u}}$.

Let us note that all correlations involving σ_t' are divided by $|\partial \bar{\sigma}_t/\partial z|$, a quantity which decreases with depth. Therefore, when energy transfer is considered, deep-water areas where σ_t' is small may contribute large terms involving σ_t' correlations.

The coherence most evident in the anti-cyclonic shear region involves the fluctuations of the two horizontal velocity components. The product $u'v'$ is negative in 56% of the cases, positive in 39% of the cases, and vanished in 5% of the cases. These statistics appear to be independent of depth. Thus for the entire water column in the anti-cyclonic region, an increase (decrease) in the eastward velocity component is accompanied by a southward (northward) deflection.

While $u'v'$ and $u'\sigma_\tau'$ were most frequently negative in the respective regions discussed above, the signs of $\overline{u'v'}$, $\overline{u'\sigma_\tau'}$, or $\overline{v'\sigma_\tau'}$ could not be determined with significance from this small ensemble. In fact, both Webster (1965) and Schmitz and Niiler (1969) report from a larger data ensemble that $\overline{u'v'}$ ispositive over the anti-cyclonic region of the Stream. It appears that the mean momentum transfer by Reynolds stresses is accomplished by intense, infrequent variations in which $u'v'$ is positive.

Figure 6a displays the structures of the σ_t and axial velocity fields during a cruise in which light water was accelerated downstream ($u'\sigma_\tau' < 0$) on the cyclonic side. Figure 6b displays these structures at the opposite phase of the oscillation, when dense-water intrusions accompany a deceleration. Here we display a situation in which, with the intrusion of the axis of the Stream toward shore, there is a depression of the entire thermocline and a deepening of the region of maximum geostrophic shear. Note that the slope of the $27\sigma_\tau$ isopycnal is larger with onshore movement of

the axis. With the decrease of nearshore flow, the counterflow underlies a greater portion of the cross-section, although its magnitude has decreased, and a geostrophic tilt of isopycnals increases at the $25\sigma_\tau$ surface. Indeed, the time history of the variability is a complicated one, full of salient scales and features which cannot be described by this set of observations. Düing (1973) describes a characteristically similar oscillation at the Miami latitude, whence the gross features of the cycle he described appear to be a common phenomena of the week-to-week variability within the entire Florida Current.

Acknowledgements. The observational aspects of this work N00014-67-A-0386-0001 were supported by Office of Naval Research Contract No.; the data analysis was carried out under National Science Foundation Grant GA 36458X. The authors are grateful to the captain and crew of the R/V Gulf Stream for their consistent performance and to Professor W. S. Richardson for his direction during and after the field program.

REFERENCES

Düing, W. 1973. Observations and first results from project SYNOPS 71. Univ. of Miami, Rosenstiel School of Marine and Atmospheric Science Scientific Report.

Düing, W., and D. Johnson. 1971. Southward flow under the Florida Current. Science, *173:* 428–430.

Düing, W., and D. Johnson. 1972. High resolution current profiling in the Straits of Florida. Deep, Sea Res., *19:* 259–274.

Lee, T. N. 1972. Spin-off eddies in the Gulf Stream. Ph.D. Thesis, Univ. of Florida, Tallahassee, Florida.

Niiler, P. P., and W. S. Richardson. 1973. Seasonal variability of the Florida Current. J. Mar. Res., *31*(3), in press.

Reinsch, C. H. 1967. Smoothing by spline functions. Numerische Mathematik, *10:* 177–183.

Richardson, W. S., and W. J. Schmitz. 1965. A technique for the direct measurement of transport with application to the Straits of Florida. J. Mar. Res., *23*(2): 172–185.

Richardson, W. S., A. R. Carr, and H. J. White. 1969. Description of a freely dropped instrument for measuring current velocity. J. Mar. Res., *27:* 153–157.

Richardson, W. S., W. J. Schmitz, Jr., and P. P. Niiler. 1969. The velocity structure of the Florida Current from the Straits of Florida to Cape Fear. Deep-Sea Res., *16* (Supplement), 225–231.

Schmitz, W. J., Jr., and P. P. Niiler. 1969. A note on the kinetic energy exchange between fluctuations and mean flow in the surface layer of the Florida Current. Tellus, *21:* 814–819.

Webster, F. 1965. Measurements of eddy fluxes of momentum in the surface layer of the Gulf Stream. Tellus, *17:* 239–245.

Received: *10 December, 1973*; revised: *25 July, 1974.*